Innovative composite sorbent for thermal energy storage based on a $SrBr_2 \cdot 6H_2O$ filled silicone composite foam

Luigi Calabrese[1,2*], Vincenza Brancato[2], Valeria Palomba[2] Andrea Frazzica[2], Luisa F. Cabeza[3]

[1] Department of Engineering, University of Messina, Messina, Italy

[2] CNR – ITAE – Istituto di Tecnologie Avanzate per l'Energia "Nicola Giordano", Salita S. Lucia sopra Contesse 5, Messina 98126, Italy

[3] GREiA Research Group, INSPIRES Research Centre, Universitat de Lleida, Pere de Cabrera s/n, 25001-Lleida, Spain

* Corresponding author: lcalabrese@unime.it

Keywords: $SrBr_2 \cdot 6H_2O$, composite foams, sorption storage, hydration, TGA

Abstract

This paper reports about the first experimental activity on a composite material for thermal energy storage, based on a $SrBr_2 \cdot 6H_2O$ filled silicone foam. The morphological and thermal features of the composite with different salt content (i.e. between 40 wt.% and 70 wt.%) were investigated. The dehydration behaviour was studied by thermo-gravimetric analysis. Furthermore, scanning electron and 3D optical microscopy were used to compare the cellular microstructure of the composite foams. The synthesized foams are characterized by a well-interconnected cellular structure with a three-dimensional porous network. This, together with the high permeability to water vapour of the matrix favours water vapour diffusion and allows the reaction of all the salt embedded in the matrix. The main advantages of the composite material were analysed and compared to other composites in literature. Since the production process, especially for higher salt content, seemed not sufficiently effective, causing a reduced foaming ration and lower ability to incorporate the salt hydrate, possible improvements were proposed and discussed.

1. Introduction

The massive research on renewable energies and their application in several fields cannot preclude from the presence of an energy storage [1]. Among the energy storage technologies, the development of thermal energy storage (TES) is considered one of the pillars in the energy vision towards 2030 or even 2050 by several international roadmaps [2–5]. Thermal energy can be stored either in the form of sensible heat, latent heat or physical and chemical reactions, the so-called thermochemical storage [6]. The main advantages of thermochemical storage compared to the others technologies are the reduced (virtually zero) thermal losses and the high energy density, up to 1 GJ/m^3 at system level [7,8]. However, research on thermochemical storage is still required, especially at materials level, due to stability and corrosion issues [9]. Among the materials suitable for thermochemical storage at low-medium temperature levels (i.e. 70-120°C), salt hydrates have been widely studied and identified as promising alternatives, due to the wide availability and high theoretical energy density. Donkers et al. [7] realised a screening on several materials in order to collect and analyse the thermodynamic data of numerous salt hydrate reactions. One of the salt hydrates that present interesting features is strontium bromide hexahydrated, $SrBr_2$ $6H_2O$. The solid-gas thermochemical reaction involving the salt is related to the following monovariant equilibrium reactions:

$$SrBr_2 \cdot 6H_2O_{(s)} \rightleftarrows SrBr_2 \cdot H_2O_{(s)} + 5H_2O_{(g)}$$

$$H_2O_{(l)} \rightleftarrows H_2O_{(g)}$$

The reactions, in a closed system, occur at temperatures lower than 100°C. For instance, Fopah-Lele et al. [10] realised the dehydration at 58 °C and hydration at 45 °C; Mauran et al. [11] realised the dehydration at 80°C and Fopah-Lele et al. worked at 89–90 °C. In an open system, dehydration can be performed in a temperature range of 60-80°C and hydration at 20-35°C [12,13]. Such temperature levels make $SrBr_2 \cdot 6H_2O$ a promising candidate for the application with solar heat and low-grade waste heat, two of the main heat sources in renewable-based systems.

Several studies have assessed the performance of such a material; recently, Fopah-Lele and Tamba [14] presented a review, highlighting the application of strontium bromide as a phase change and thermochemical material for solar energy storage in different sectors and reporting the main thermo-physical characteristics of the material (melting temperature, kinetics, sorption and heat storage capacity, thermal conductivity, permeability).

Two of the main limitations to a wider application of $SrBr_2 \cdot 6H_2O$ are the high cost and the performance degradation with cycling. In order to tackle the former issue, Gilles et al [15] proposed a cost-effective industrial scale method of production of $SrBr_2$. The experimental investigation allowed the synthesis of material with a purity up to 97.6% with an expected cost of 0.09-0.28 €/kWh of heat stored, further proving the potentiality of the material also from an economic point of view.

Concerning the latter issue, performance degradation is generally due to the swelling of the salt, due to a change of crystal structure, or the agglomeration of partially salt hydrate, especially in small-scale samples [10]. Instead, problems of aggregation or pulverization are observed when the salt is used in a thermochemical storage reactor [16,17]. One solution generally proposed is the realisation of composite materials with porous matrices [18,19]. For instance, in [20] the performance of $CaCl_2$ composites for thermochemical storage are examined. Silica-gel, alumina, and bentonite were chosen as supports. Among the composites, the ones with silica gel showed the best sorption properties. Zeolite has also been studied as a matrix, as in [21], where composites with $MgSO_4$ and zeolites were studied for seasonal storage applications. Some studies are reported in literature regarding composites with strontium bromide. Recently, Cammarata et al. [22] proposed the use of natural graphite as a support to hold the salt. The results showed that the natural graphite could improve the hydration-de-hydration kinetics by reducing hysteresis and increase the thermal conductivity of the material. More recently, Salviati et al. [23] proposed the addition of an organic compound, PDAC, polydiallyldimethylammonium chloride, to the strontium bromide/graphite composites. Experimental outcomes of the investigation show that PDAC has a beneficial effect on water sorption and mechanical resistance upon hydration/dehydration cycling.

Such results indicate the need for new formulation of composite materials for thermochemical storage, able to act not only on the sorption capacity and kinetics, but also on the mechanical resistance and corrosion problems that might arise when using such a material [24]. The solution proposed and investigated in the present paper is the realisation of composites using a flexible matrix, i.e. a silicone foam, according to an approach already exploited for use with zeolites and $MgSO_4$ in sorption chiller/heat pumping and storage applications [25–28]. In the present paper, the experimental activity of a composite based on a silicone foam embedding $SrBr_2 \cdot 6H_2O$ is presented for the first time. Morphological and thermal properties were investigated, with the aim of evaluating the feasibility of the material for thermal energy storage applications. A morphological analysis of composite foams at varying salt hydrate amount was carried out, in order to assess the effect of salt addition in the microstructure porosity and foaming process. Based on digital image analysis, size and shape of bubble distribution were calculated and related to material preparation. The thermal behaviour was addressed by studying the dehydration performance analysis with a thermo-gravimetric apparatus. The so-obtained results on composite foams were compared with other composites with the same salt hydrate, reported in the literature, in order to highlight advantages and issues of this class of material and to identify possible research and development future strategies.

2. Materials and methods

The composite silicone foams, based on poly(methylhydrosiloxane) (PMHS, molecular weight 1,400-1,800, cas: 63148-57-2) and a silanol terminated polydimethylsiloxane (PDMS, molecular weight 18,000, cas: 70131-67-8) compounds, filled with different percentages of $SrBr_2 \cdot 6H_2O$ salt hydrate were obtained according to the procedure described in [29]. The synthesis of the silicone matrix was carried out mixing poly(methylhydrosiloxane) $(CH_3(H)SiO)_n$ as monomer, silanol terminated polydimethylsiloxane as hardener, with bis(2-ethylhexanoate)tin (molecular weight 405.11, cas: 301-10-0) as catalyst (all supplied by Gelest Inc., Morrisville, USA).

The $SrBr_2 \cdot 6H_2O$ salt hydrate was slowly added in different percentages (ranging from 40-70 wt.%) in the siloxane matrix, under vigorous mixing until a homogeneous slurry was obtained. Finally, the foaming reaction was performed in an oven under controlled temperature (60°C for 24 h). Figure 1 summarizes the preparation procedure.

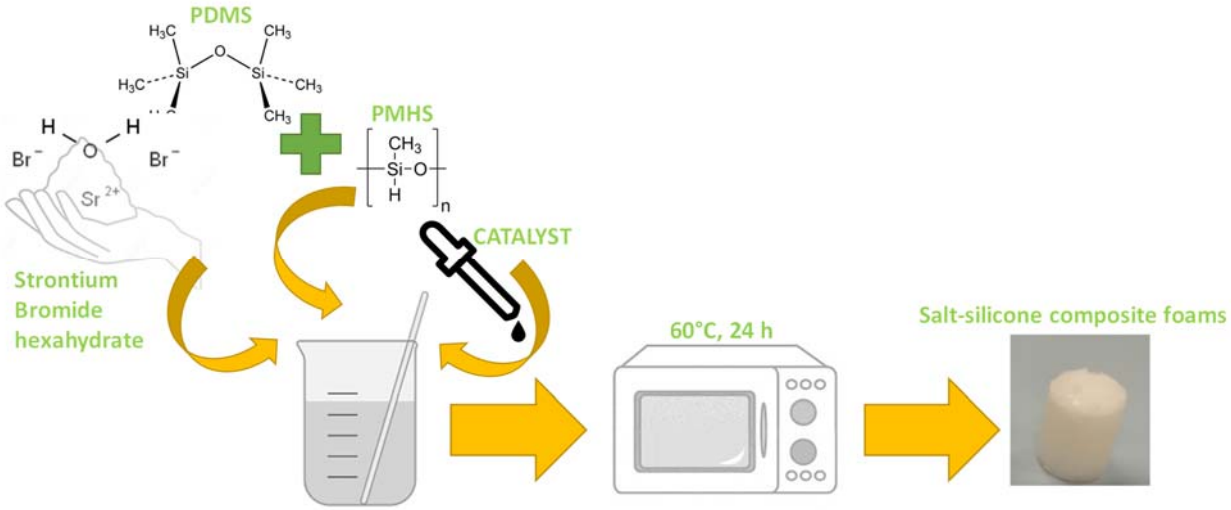

Figure 1: Scheme of the preparation steps of the salt-silicone foams

The siloxane matrix was chosen considering its excellent water vapour permeability [30], in order not to inhibit the water vapour mass diffusion process or a modification of the de/hydration process during the operation.

Figure 2 shows the composite foam samples obtained at increasing salt content (in the range 40 wt.%-70 wt.%).

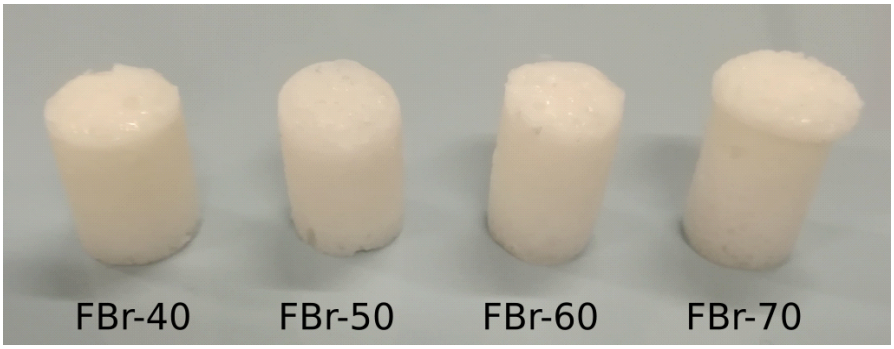

Figure 2: Composite foam samples at increasing SrBr2·6H2O content (from 40 wt.% to 70 wt.%)

The composite foams were classified with the code "FBr-" followed by a number indicating the $SrBr_2 \cdot 6H_2O$ salt hydrate content in weight percentage (wt.%),e.g. the code "FBr-40" refers to a composite foam constituted by 40 wt.% of salt hydrate filler. As reference, also a foam of pure silicone, without salt hydrate (FBr-0) was prepared.

Morphological analysis

Morphological characterization of the composite foams were carried out by scanning electron microscopy (SEM instrument Philips XL-30-FEG) and 3D optical digital microscopy (Hirox HK-8700).

In order to better investigate the effect of the salt hydrate content on the morphological characteristics of the composite foam, image processing of the composite foams was carried out. The proposed method consists in determining the distribution of porosities on contiguous and slightly overlapping high-resolution images of the entire cross section of the foam, obtained by means of tiling image reconstruction procedure provided by the Hirox 3D microscope HK-8700. Such image processing was employed in order to minimize calculation error and optimize the statistical parameters related to population data [31]. Since the images did not have uniform contrast, it was not possible to effectively apply an automatic evaluation criterion for bubble edges discrimination from the composite framework, but a semi-automatic- procedure was applied. In particular, for all the foam batches, the border for each bubble was manually tailored from cross-section image by using a photo-editor program (Gimp 2.8). Afterwards, for each sample, the whole bubble perimeters distribution was analysed, by means of an image analysis software (ImageJ 1.48, WS Rasband, ImageJ, US National Institutes of Health). The geometrical information on the foam morphology was used as input for statistical analysis on the frequency distributions of population of data. The frequency distribution of bubbles was performed, clustering the bubble size population data into well-defined histogram classes according to Sturges rule [32], where the number and the intervals of the classes (Nc and w, respectively) were defined according to the following equations:

$$\mathrm{Nc}=3.322\log N_b + 1 \tag{1}$$

$$\mathrm{w}=\frac{d_{\max} - d_{\min}}{N_c} \tag{2}$$

where N_b is the amount of bubbles, d_{min} and d_{max} are smallest and largest measured bubble diameters, respectively.

Thermogravimetric analysis

The pure salt and the polymeric composite foams were characterized by means of thermo-gravimetric analysis (TGA), performed by Netzsch Thermische Analyse TASC 414/2. The measurements were carried out according to the following procedure: 10/15 milligrams of pristine salt ($SrBr_2 \cdot 6H_2O$) or foam at varying salt content (FBr-40 and FBr-70) were weighed with microbalance and placed inside the measurement apparatus. Afterwards, a heating ramp between 25°C and 300°C, with a heating rate of 1°C/min under nitrogen flow (50 ml/min), was carried out, in order to follow the dehydration process of the salt. For each specimen, different pieces of the foams were tested, in order to evaluate the distribution of the salt along the vertical direction of the foams. In particular, three fragments, removed from top, middle and bottom area of the foam, were selected to assess if sedimentation occurs and if this influences the dehydration phenomena and TES performance of the foams.

Compression tests

Test specimens (dimension 10x10x10 mm^3) were obtained by cutting from moulded cylinder foams. Parallelism of top and bottom surfaces was ensured by optical microscopy by using a 3D digital microscope (Hirox HK-8700). Three compression tests for each batch were carried out at room temperature, according to [26], by using a universal testing machine (2.5kN Zwick Line) equipped with a 2.5 kN load–cell (sensitivity of 0.001 N). Crosshead speed was 1.0 mm/min.

Table 1 presents the details of the applied design of experiment (DoE).

Table 1: Details of the applied design of experiment

	Samples	*Thermo-gravimetric analysis*			*Compression*	*Morphological*
		Top	*Middle*	*Bottom*	*Test*	*Analysis*
FBr-0/70	2	2	2	2	3	2

3. Results and Discussion

3.1 Morphological analysis

Preliminarily, some information, concerning foaming process and bubble distribution in the composite foams, was acquired analysing the cross-section of the samples (50x magnification), by means of a 3D optical microscope (see Figure 3). The plain of view is parallel to the foaming direction, indicated by a red arrow (from bottom toward the top) in Figure 3.

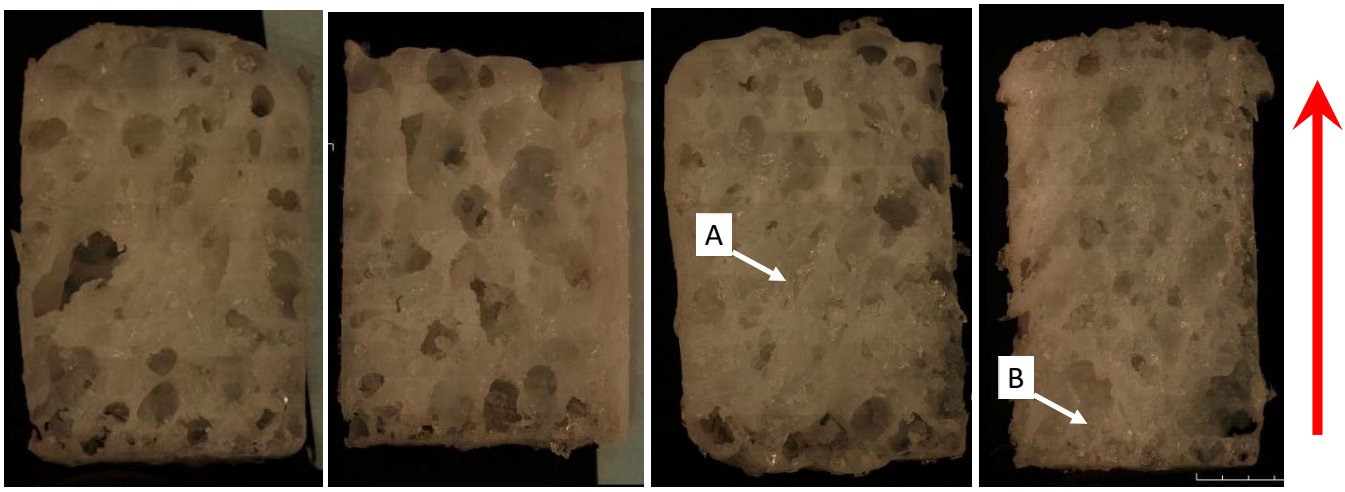

a) b) c) d)

Figure 3: 3D optical images of a) FBr-40 b) FBr-50 c) FBr-60 d) FBr70 composite foam samples. Red arrow indicates the foaming direction.

All the samples show a well-defined foamed structure. The bubbles are homogenous and randomly distributed along the whole cross section. Furthermore, a mixed open/closed cell morphology, with good interconnection channels among bubbles, can be identified. The foaming phenomenon in the structure can be ascribed to the dehydrogenative reaction between the two siloxane compounds used as matrix constituents.-Indeed, according to [27], hydroxyl and hydride reactive groups of PDMS and PMHS siloxane compounds, respectively, are able to react generating a siloxane Si-O-Si bond that eventually leads to three-dimensional cross-linked network. At the same time, volatile gaseous hydrogen molecules, obtained as reaction product, act as foaming agent. During the foaming process, activated by thermal treatment, the bubbles grow up and coalesce providing macro and micro pathways in the three-dimensional porous network.

This foamed structure, branched and interconnected, plays a key role in the water vapor diffusion during the hydration and dehydration phases, facilitating mass transport phenomena. A three-dimensional network of contiguous paths for vapor diffusion can be observed both for low and high salt content.

When increasing the salt content however, there is a slight reduction in foaming, as shown by the reduction of the average bubble size. This behavior can be justified considering that, as the salt content increases, there is a progressive increase in the viscosity of the composite slurry. Consequently, during the chemical and physical foaming process of the foam the bubble growth and coalescence phenomena are hindered [33]. This leads to the formation of bubbles with a small average diameter. Despite this, the foam is still porous and characterized by a well-shaped cellular structure. At the

same time, a reduction in the capacity to incorporate the salt hydrate filler can be highlighted for higher salt content.

The FBr-40 and FBr-50 foams show a good interaction between the various constituents. The filler is effectively embedded in the silicone matrix. On the other hand, foams with a high salt content, FBr-60 and FBr-70, show superficial efflorescence phenomena that can be associated with the agglomeration of salt hydrate crystals (point A in Figure 3). For these salt percentage, the inclusion of the salt hydrate in the silicone matrix is less effective, suggesting a limited cohesion between the constituents.

Furthermore, a sedimentation phenomenon can be highlighted. This phenomenon leads to the formation of a thin, compact and dense salt hydrate layer at the bottom of all samples (point B in Figure 3). The sedimentation of the salt hydrate - and the consequent gradient of concentration along the foaming direction - represent an aspect that must be carefully considered since it can lead to foam heterogeneity and can involve discrepancies in the efficiency of the hydration and dehydration cycles. Consequently, it will be further investigated with thermo-gravimetric tests.

In order to clarify the effect of the addition of the salt hydrate on the morphological characteristics of the composite foam, a statistical analysis of the bubble distribution on the porous structure was carried out. Table 1 reports some representative statistical parameters for the various samples produced.

Table 2: Main statistical parameters on bubble size distribution of salt hydrate composite foams

	FBr-0	*FBr-40*	*FBr-50*	*FBr-60*	*FBr-70*
Salt hydrate [wt.%]	0.0	40.0	50.0	60.0	70.0
Diameter [mm]	2.27	1.94	1.91	1.68	1.37
Standard Deviation (SD)	2.10	1.10	1.10	0.91	0.92
Coefficient of Variance (CoV)	0.93	0.57	0.58	0.54	0.56
Circularity	0.62	0.63	0.61	0.56	0.55

Standard deviation (SD) and Coefficient of variance (CoV) were used to assess the data distribution and homogeneity. A low or high SD value indicates that the data points tend to be close or far away from the average value of the data set, respectively. However, a more effective parameter, useful for data set with different average value is the CoV parameter. This is a dimensionless value able to obtain a statistically more representative parameter to evaluate the variability of the data with respect to its average. Finally, the circularity, C, is calculated, according to the following equation

$$C = 4\pi \times \frac{(Area)}{(Perimeter)^2} \tag{3}$$

where C is a parameter that is equal to 1.0 for circular shaped bubbles and tends to 0.0 for irregular ones.

Analysing the data reported in Table 1, it is possible to notice that there is a progressive reduction of bubble diameter at increasing salt content. However, the negligible variation of standard deviation and coefficient of variance indicate that the samples are characterized by a common heterogeneity. This trend can be justified considering that at increasing filler content, due to higher slurry viscosity, the bubble coalescence is progressively hindered. For composite foams with low salt hydrate content, the coalescence phenomenon, occurring during the foaming stage, leads to a homogeneous large bubble distribution. Vice versa, for composite foams with high salt hydrate content, a smaller bubble distribution was observed. At the same time, the low circularity values calculated for FBr-60 and FBr-70 foams indicate a smaller dimension of the bubbles of the foam, probably due to incomplete coalescence phenomenon [29].

These considerations are summarized in Figure 4, which shows the evolution of diameter and circularity of the bubbles at increasing salt content. A clear transition region at a filler content of 50 wt.% can be identified: above this threshold, a reduction of bubble diameter and a significant reduction of circularity were observed. This phenomenon can be related to the higher salt hydrate amount in the composite that induces a higher viscosity of the slurry. In turn, this limits the coalescence of the bubbles and the blowing up of the foam. The consequence is a cellular structure with interconnected bubbles that not have not completed their coalescence, as confirmed by the reduced diameter.

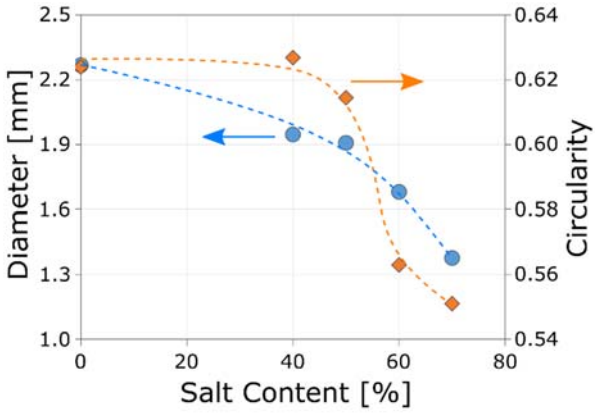

Figure 4: Average cell size diameter and circularity at increasing salt hydrate content

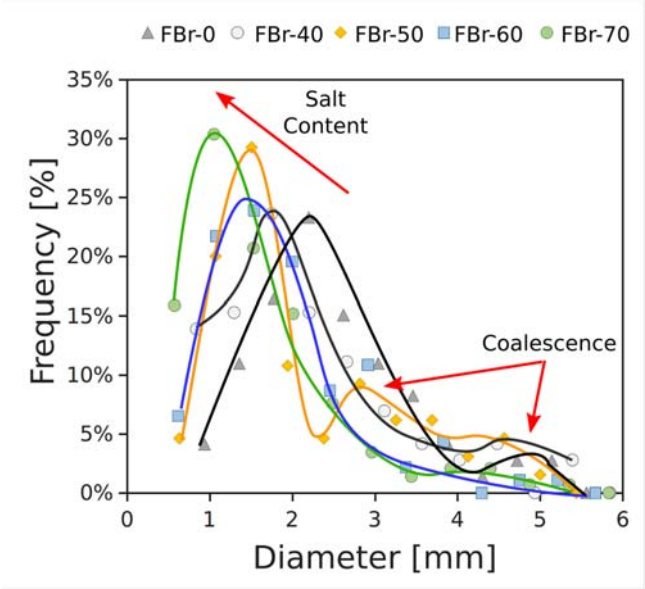

Figure 5: Frequency plot of diameter distribution for all the foams

More information about the microstructure and the influence of the composite formulation on such an aspect can be gathered by analysing the distribution of diameter frequency, reported in Figure 5. For the composites with low salt hydrate content (FBr-40 and FBr-50), two peaks can be identified. The first one at a small diameter, in the range 1.5-2.0 mm, can be ascribed to the new born bubbles, during the foaming stage, that do not have time to coalesce. The other peak is at about 5.0 mm diameter, due to the large coalescence of bubbles. For salt content above 50 wt.% the frequency distribution of bubble diameters is characterised by only one relevant peak at low diameters. This behaviour is due to the limited coalescence phenomena in the high viscous slurry. Subsequently, for FBr-60 and FBr-70 samples, the coalescence peak is depressed. At the same time, an evident shift towards lower bubble size of the first large peak takes place. Furthermore, the higher peak at low diameter increases in magnitude at lower salt content, indicating that a large amount of bubble at low diameter are present.

Scanning Electron Microscopy (SEM) analysis was carried out to better highlight salt distribution in the silicone foam.

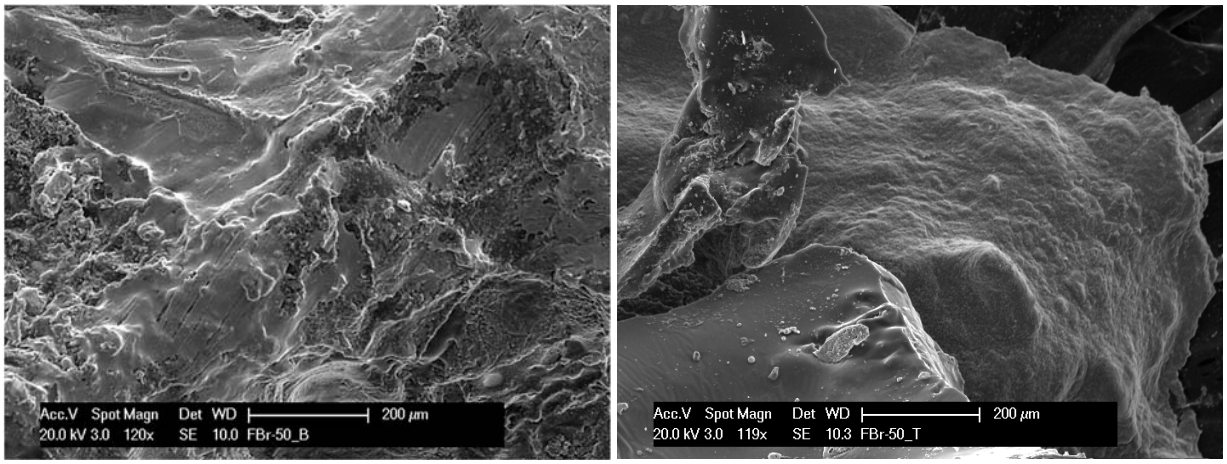

Figure 6: Micrographs of samples FBr-50 bottom (left) and FBr-50 top (right)

Micrographs of FBr-50 bottom and top samples are shown in Figure 6, on the left (FBr-50_B) and on the right (FBr-50_T), respectively. The morphology of the two samples is quite different. The FBr-50_B shows a rough surface with several ripples and some voids, probably due to physical or chemical foaming phenomena in the foam. The amount of salt is high in this area but it is not uniformly distributed inside the matrix. Indeed, it is perfectly embedded in the smooth region while grains are visible in the other regions. The lack of a continuous layer of matrix over the salt and its high content in this area could justify the abundant leakage of the filler from the matrix during hydrothermal cycling or during handling. On the other hand, the micrograph of FBr-50_T shows an extended smoothed area, indicating the presence of a homogeneous silicone shell that cover all external surface. Nonetheless, a lower amount of filler than in the sample from the top side can be identified. Indeed, only a conglomerate of salt crystals set in matrix is visible in the central area of the figure. The cell wall without filler is visible in the background of the micrograph.

Therefore, despite the high filmogeneity of the polymer matrix, the salt hydrate grains are not perfectly encapsulated in the foam structure, probably due to their stratification along the foaming direction.

Compression tests

Table 3: Compressive elastic Modulus at increasing salt hydrate content of the composite foams

	Compressive elastic Modulus [MPa]	*Standard deviation*
FBr-40	2.8*10-2	0.007
FBr-50	4.9*10-2	0.009
FBr-60	5.1*10-2	0.010
FBr-70	5.7*10-2	0.011

In order to better understand the potential applicability of this class of materials for TES applications, a more effective assessment of the correlation between morphology and mechanical properties is needed. Table 3 shows a preliminary comparison of the compressive elastic moduli of composite foams at increasing salt hydrate content. The addition of the filler causes a progressive increase of stiffness. FBr-70 foam has an elastic modulus of 5.7*10-2 MPa, about double than composite foams with lower salt amount (FBr-40 foam). This behavior can be related to the foam morphology and its cell wall structure, considering that the elastic modulus of composite foams increase with increasing cell wall thickness [34]. At the same time, a gradual increase of standard deviation can be observed at increasing filler content in the composite foam formulation. This statistical information, directly confirms the stratification issue discussed in the previous sections. The interesting results obtained indicate that it is possible to evaluate the foam homogeneity by investigation of the mechanical properties modification. In such a context, a complete testing campaign is ongoing and the results will be presented in a further work, in order to assess the optimal combination of stress, strain and mechanical energy adsorption.

3.2 Thermogravimetric analysis

With the purpose to better evaluate dehydration phenomena occurring on the pure salt and on the composite foams, thermo-gravimetric analysis (TGA) was carried out.

According to literature results [22,35], the pure $SrBr_2 \cdot 6H_2O$ clearly shows a two steps dehydration process. Indeed, five water molecules are removed from the salt during the first step (between ambient temperature and about 80°C), while one water molecule is lost in the second dehydration step (before of 180°C). The total weight loss of the pure salt is equal to 29%, in close agreement with the literature data [22,36,37].

The pure silicone foam, without salt addition, shows an inert behavior to water dehydration phenomena indicating a negligible weight loss in the whole range of analysis [28]. Consequently, considering the negligible loss of mass that can be associated with the siloxane matrix, the weight loss evolution, observed for all the composite samples, can be ascribed exclusively to the dehydration phenomenon of $SrBr_2 \cdot 6H_2O$ salt hydrate.

Due to the stratification of various layers at different salt contents along the foaming direction, as found by means of 3D optical microscopy and SEM images, it is plausible to consider that the total amount of salt hydrate is divided unevenly into three different areas (bottom, middle and top, see Figure 7). The consequence of the stratification phenomenon is that the mass loss is significantly influenced by the specimen location. For this reason, three specimens have been tested, removed from bottom (sample A), middle (sample B) and top (sample C) area, respectively. In particular, both for

FBr-40 and FBr-70, the specimen extracted from the bottom area, along the foaming direction (Figure 7), showed the highest salt amount and thus the maximum percentage of dehydration. Vice versa, the specimen removed from top shows the lowest salt content and thus the minimum dehydration capacity. It is important to point out that the evolution of dehydration phenomenon of the polymeric composite foams always shows the two dehydration steps described above.

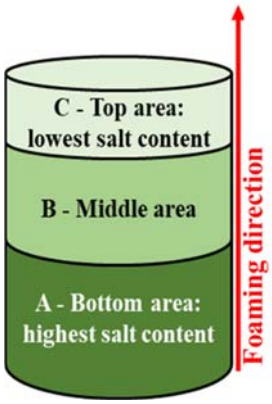

Figure 7: Stratification of salt content along the foaming direction

Figure 8 (a-b) summarizes the results for two reference samples, FBr-40 and FBr70, as well as the pure salt.

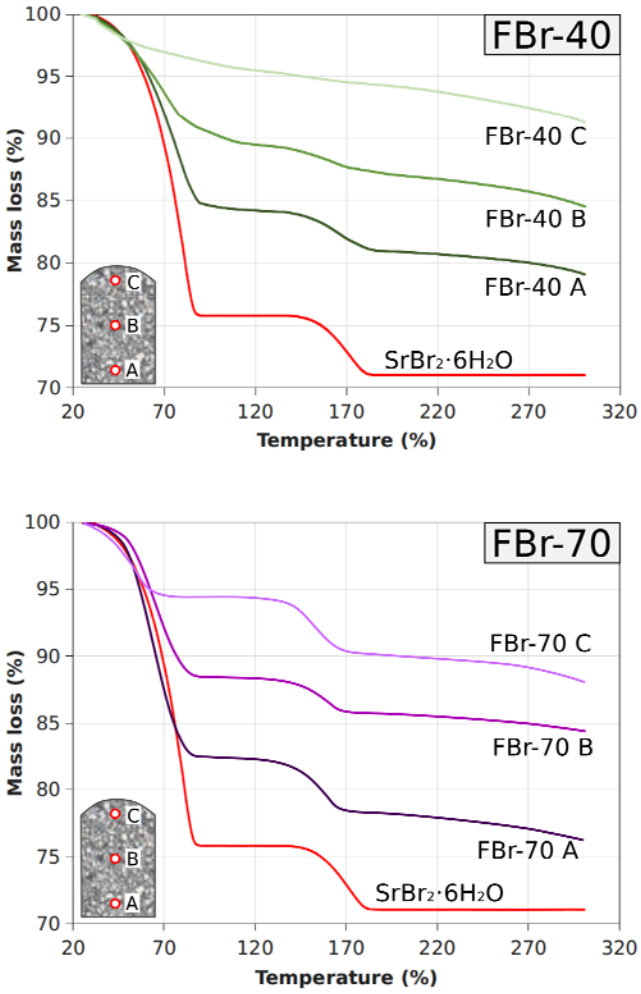

Figure 8: Thermo-gravimetric dehydration curves: (a) weight loss, dm/m0; (b) first derivate of the weight loss, DTG

The sample called FBr-40 A evidenced a maximum weight loss of 20.9 wt.%. This result indicates that the salt hydrate, added to the composite foam as filler, is able to release water molecules and activate the dehydration process. Consequently, although the $SrBr_2 \cdot 6H_2O$ salt is embedded in the silicone foam, the silicone matrix does not inhibit or hinder the water dehydration. Thanks to the high permeability of polymeric component, the evaporation process takes place effectively [38].

A progressive reduction of mass loss can be observed for samples located towards the top area of the specimen (15.5 wt.% and 8.7 wt.% for sample FBr-40 B and FBr-40 C, respectively). This behavior can be ascribed to a lower content of salt hydrate in the foam portions. Anyway, despite the sedimentation phenomenon the average content of the filler in the three considered areas is close to 40 wt.%.

Based on the weight loss at different heights, the distribution of the salt content was calculated as the ratio between the weight loss of the considered specimen in a particular area and the total weight loss

(i.e., the sum of three losses of all the areas). The values for the sample FBr-40 are 19.3%, 34.4% and 46.3% for top, middle and bottom zone, respectively.

A similar behavior can be observed for the FBr-70 sample. In this case, the maximum weight loss measured is 23.9 wt.% (sample FBr-70A), due to the higher amount of salt in the foam. In the other regions, the total weight loss was 15.7 wt.% and 12.0 wt.%, respectively. In this case, it is evident that the average value of weight loss is not compatible with a filler content of 70 wt.%. Considering the obtained value, it seems that the total amount of $SrBr_2 \cdot 6H_2O$ is equal to about 60 wt.%. This can be explained according to what reported in [28], in which it was demonstrated that a small amount of filler is lost during the manipulation of the samples and during the withdrawal of the tested specimen. As observed for the sample FBr-40, the higher weight loss occurs in the specimen located at the bottom. Indeed, in this case, sedimentation is much more evident than for the FBr-40 foam and a significant difference between the bottom and middle/top region can be identified: about half of the overall amount of salt inside the specimen is located at the bottom (46.4%), whereas 30.4% is in the middle and 23.3% in the uppermost sample. Such results are summarized in Table 4.

Table 4: total weight loss at 180°C and calculated salt distribution in the composite foam along vertical axis.

	FBr-40			***FBr-70***		
	Top	***Middle***	***Bottom***	***Top***	***Middle***	***Bottom***
Theoretical salt hydrate [wt.%]	40.0	40.0	40.0	70.0	70.0	70.0
Total weight loss [%]	8.7	15.5	20.9	12.0	15.7	23.9
Salt hydrate distribution [%]	19.3	34.4	46.3	23.3	30.4	46.4

3.3 Feasibility of the composites for thermal energy storage application and future developments

The salt hydrate chosen for the present analysis has been widely investigated in the literature, both for thermochemical and latent storage [14], thanks to its melting/reaction temperature below 100°C. To overcome the limitations in heat and mass transfer of the pure salt, different composites were proposed. However, most of the activities reported in literature focus on the thermal performance of the material. For instance, the expanded graphite- salt hydrate composites proposed by Zhao et al.

[37] showed an increased heat transfer, if compared to the pure salt, but a limitation in mass transfer. Zhang et al. [36] analysed $SrBr_2$-expanded vermiculite composites and stated their potential for low temperature thermal energy storage based on the calculation of the volumetric energy density at material level, but the results from DSC analysis clearly indicate that the increase in the sorption enthalpy of the composites does not grow linearly with the increase in the mass concentration of salt solution and indeed the differences between the various cases are low. Such a behaviour is ascribed to the limitations in mass transfer since composites with higher content of salt results in more compact and dense blocks, that represent increased obstacles to mass and heat transfer. In the work reported by Salviati et al. [23], the composites made with the salt hydrate, expanded natural graphite and polydiallyldimethylammonium chloride show good heat and mass transfer properties, but the mechanical resistance of the material proved to be a critical issue: severe damage in the form of cracks to the composite tabs occurred already after the first hydration/dehydration cycle. In another study by D'Ans et al. [39], a strong humidity dependence of thermal and mass transport properties of composites based on $CaCl_2$ encapsulated in microporous silica gel was evidenced: considering the small dimensions of the pores of the matrix, for high humidity values (i.e. as the material approaches the "charged" state, a strong reduction in mass transfer occurs, due to the blockage of the pores by the adsorbate.

Such results prove that, despite the great efforts and the potentiality of the material, still work is needed at material level, in order to obtain a reliable composite that really allows exploiting the interesting features of strontium bromide, overcoming at the same time heat and mass transfer limitations and mechanical damaging with cycles. Future investigations on the developed composite sorbent will be also performed in order to comparatively investigate, against materials already investigated and reported in the literature, the achievable energy storage performance under real boundary conditions, as reported in [40].

The composite here proposed does not pose any mass transfer limitation, due to the peculiar nature of the matrix, that has a high permeability to water vapour and, while supporting the salt provides a three-dimensional network of preferential path for water vapour diffusion that allows the reaction of all the salt embedded in the matrix. At the same time, mechanical problems that might arise from the stresses due to the vapour pressure and the expansion/contraction of the salt during cycling are prevented by the flexibility of the polymeric matrix. Indeed, a future experimental activity will be carried out to assess the mechanical behaviour of the composites under several compression/dilatation cycles and the correspondent effect on the sorption and thermal behaviour of the material proposed. The heat transfer performance of the composite can be increased, still keeping the benefits of the

approach in the design of the matrix-filler chosen, by adding conductive particles to the formulation that allow creating also a thermal network for heat transfer [41].

Nonetheless, the production of the samples and their morphological analysis indicated that an improvement in the formulation and realisation of the composites is needed to avoid sedimentation in the slurry during preparation. Indeed, the distribution of the salt in the vertical direction was uneven, especially for the composites with higher salt content. This is a serious issue, since the distribution of the salt influenced also the thermal behaviour of the composite and might represent an even more significant issue in the realisation of a prototype. The concentration of salt in one zone can indeed lead to the necessity of a higher heat rate in one part of the heat exchanger, thus forcing the need for oversized and bulkier components. In addition, the concentration of water molecules that cannot be exchanged can cause degradation of the material and components.

However, a modification in the formulation of the polymer for the matrix could prevent such phenomenon. The sedimentation phenomenon is mainly due to the hydrophilic nature of the salt and hydrophobic behaviour of the silicone foam. This leads to an immiscible mixture without a chemical interaction between filler and matrix and therefore a sedimentation of the salt, which is faster for higher salt amount.

In order to limit this aspect, a possibility that will be investigated in the future is the use of a PDMS matrix with a less pronounced hydrophobic behaviour, which can improve the chemical compatibility between the support and the salt hydrate filler, thus leading to a more homogeneous composite foam [42,43].

4. Conclusions

The present paper focuses on the first experimental activity on a composite for thermochemical storage of low-grade heat, e.g. from renewable sources. The material proposed and produced is based on a silicone foam that supports $SrBr_2 \cdot 6H_2O$ as storage material, with the aim of reducing the degradation of the salt with cycling, as well as the reduction of mechanical properties. The size, circularity and distribution of bubbles were analysed by means of optical microscopy, showing that a three-dimensional network of interconnected paths for water vapour diffusion exists. Such findings were confirmed by TGA analysis that found results consistent with other referenced materials. The production process was found to have a great influence on the distribution of the salt along the samples, since the high viscosity of the slurry induced a concentration of the salt at the bottom of each sample. The results obtained were analysed and compared with other composites with the same salt hydrate in the literatures and possible strategies for a future development of materials with more homogeneous structures and properties were proposed. The development and optimization of such a

kind of TES material could be a viable solution both for long- and short-term storage applications, in domestic and industrial processes, thanks to the simplicity of the manufacturing process and the flexibility that allows the production of TES of different size.

Acknowledgements

This work was partially funded by the Ministerio de Ciencia, Innovación y Universidades de España (RTI2018-093849-B-C31).. Dr. Cabeza would like to thank the Catalan Government for the quality accreditation given to her research group (2017 SGR 1537). GREiA is certified agent TECNIO in the category of technology developers from the Government of Catalonia. This work is partially supported by ICREA under the ICREA Academia programme.

References

[1] Stratego, Low-Carbon Heating and Cooling Strategies for Europe - Final Publishable Report of the EU-funded project STRATEGO, (2016) 40.

[2] European Commission, Energy roadmap 2050 Energy, (2012). doi:10.2833/10759.

[3] L.F. Cabeza, E. Galindo, C. Prieto, C. Barreneche, A. Inés Fernández, Key performance indicators in thermal energy storage: Survey and assessment, Renew. Energy. 83 (2015) 820–827. doi:10.1016/J.RENENE.2015.05.019.

[4] Energy Agency's Energy Technology Policy Division, Technology Roadmap: Energy storage, 2014.

[5] ADEME, Energy storage systems - strategic roadmap, n.d.

[6] M. Segarra, C. Barreneche, A. Calderón, A.I. Fernández, Materials Selection for Thermal Energy Storage Applications—Case Studies, in: A. Frazzica, L.F. Cabeza (Eds.), Recent Adv. Mater. Syst. Therm. Energy Storage- An Introd. to Exp. Charact. Methods, Springer, 2019: pp. 55–66. doi:10.1007/978-3-319-96640-3_5.

[7] P.A.J. Donkers, L.C. Sögütoglu, H.P. Huinink, H.R. Fischer, O.C.G. Adan, A review of salt hydrates for seasonal heat storage in domestic applications, Appl. Energy. 199 (2017) 45–68. doi:10.1016/j.apenergy.2017.04.080.

[8] L. Scapino, H.A. Zondag, J. Van Bael, J. Diriken, C.C.M. Rindt, Sorption heat storage for long-term low-temperature applications: A review on the advancements at material and prototype scale, Appl. Energy. 190 (2017) 920–948. doi:10.1016/j.apenergy.2016.12.148.

[9] T. Brünig, K. Krekić, R. Pietschnig, Survey of dilution or adsorption enthalpies of a series of hygroscopic sorption materials, J. Energy Storage. 18 (2018) 171–174. doi:10.1016/J.EST.2018.04.028.

[10] A. Fopah Lele, F. Kuznik, O. Opel, W.K.L. Ruck, Performance analysis of a thermochemical based heat storage as an addition to cogeneration systems, Energy Convers. Manag. 106 (2015) 1327–1344. doi:10.1016/J.ENCONMAN.2015.10.068.

[11] S. Mauran, H. Lahmidi, V. Goetz, Solar heating and cooling by a thermochemical process. First experiments of a prototype storing 60 kW h by a solid/gas reaction, Sol. Energy. 82 (2008) 623–636. doi:10.1016/j.solener.2008.01.002.

[12] F. Marias, P. Neveu, G. Tanguy, P. Papillon, Thermodynamic analysis and experimental study of solid/gas reactor operating in open mode, Energy. 66 (2014) 757–765. doi:10.1016/J.ENERGY.2014.01.101.

[13] B. Michel, N. Mazet, P. Neveu, Experimental investigation of an innovative thermochemical process operating with a hydrate salt and moist air for thermal storage of solar energy: Global performance, Appl. Energy. 129 (2014) 177–186. doi:10.1016/J.APENERGY.2014.04.073.

[14] A. Fopah-Lele, J.G. Tamba, A review on the use of SrBr2·6H2O as a potential material for low temperature energy storage systems and building applications, Sol. Energy Mater. Sol. Cells. 164 (2017) 175–187. doi:10.1016/J.SOLMAT.2017.02.018.

[15] D. Gilles, T. Segato, E. Courbon, M. Degrez, P. D'Ans, Affordable Process for the Production of Strontium Bromide Used in Low Grade Heat Recovery Applications, Procedia CIRP. 69 (2018) 383–388. doi:10.1016/J.PROCIR.2017.11.056.

[16] A.-J. De Jong, F. Trausel, C. Finck, L. Van Vliet, R. Cuypers, Thermochemical heat storage – system design issues, Energy Procedia. 48 (2014) 309–319. doi:10.1016/j.egypro.2014.02.036.

[17] P.A.J. Donkers, L. Pel, O.C.G. Adan, Experimental studies for the cyclability of salt hydrates for thermochemical heat storage, J. Energy Storage. 5 (2016) 25–32. doi:10.1016/j.est.2015.11.005.

[18] A. Frazzica, V. Brancato, V. Palomba, S. Vasta, Sorption Thermal Energy Storage, in: A. Frazzica, L.F. Cabeza (Eds.), Recent Adv. Mater. Syst. Therm. Energy Storage- An Introd. to Exp. Charact. Methods, Springer, 2019: pp. 33–54. doi:10.1007/978-3-319-96640-3_4.

[19] O. Skrylnyk, E. Courbon, N. Heymans, M. Frère, J. Bougard, G. Descy, Performance characterization of salt-in-silica composite materials for seasonal energy storage design, J. Energy Storage. 19 (2018) 320–336. doi:10.1016/J.EST.2018.08.015.

[20] A. Jabbari-Hichri, S. Bennici, A. Auroux, CaCl2-containing composites as thermochemical heat storage materials, Sol. Energy Mater. Sol. Cells. 172 (2017) 177–185. doi:10.1016/j.solmat.2017.07.037.

[21] D. Mahon, G. Claudio, P. Eames, A study of novel high performance and energy dense

zeolite composite materials for domestic interseasonal thermochemical energy storage, Energy Procedia. 158 (2019) 4489–4494. doi:10.1016/J.EGYPRO.2019.01.763.

[22] A. Cammarata, V. Verda, A. Sciacovelli, Y. Ding, Hybrid strontium bromide-natural graphite composites for low to medium temperature thermochemical energy storage: Formulation, fabrication and performance investigation, Energy Convers. Manag. 166 (2018) 233–240. doi:10.1016/J.ENCONMAN.2018.04.031.

[23] S. Salviati, F. Carosio, G. Saracco, A. Fina, S. Salviati, F. Carosio, et al., Hydrated Salt/Graphite/Polyelectrolyte Organic-Inorganic Hybrids for Efficient Thermochemical Storage, Nanomaterials. 9 (2019) 420. doi:10.3390/nano9030420.

[24] P. D'Ans, E. Courbon, M. Frère, G. Descy, T. Segato, M. Degrez, Severe corrosion of steel and copper by strontium bromide in thermochemical heat storage reactors, Corros. Sci. 138 (2018) 275–283. doi:10.1016/J.CORSCI.2018.04.020.

[25] L. Calabrese, L. Bonaccorsi, P. Bruzzaniti, A. Frazzica, A. Freni, E. Proverbio, Adsorption performance and thermodynamic analysis of SAPO-34 silicone composite foams for adsorption heat pump applications, Mater. Renew. Sustain. Energy. 7 (2018) 24. doi:10.1007/s40243-018-0131-y.

[26] L. Calabrese, L. Bonaccorsi, P. Bruzzaniti, G. Gullì, A. Freni, E. Proverbio, Zeolite filled siloxane composite foams: Compression property, J. Appl. Polym. Sci. 135 (2018) 46145. doi:10.1002/app.46145.

[27] L. Calabrese, L. Bonaccorsi, A. Freni, E. Proverbio, Silicone composite foams for adsorption heat pump applications, Sustain. Mater. Technol. 12 (2017) 27–34. doi:10.1016/j.susmat.2017.04.002.

[28] V. Brancato, L. Calabrese, V. Palomba, A. Frazzica, M. Fullana-Puig, A. Solé, et al., MgSO4·7H2O filled macro cellular foams: An innovative composite sorbent for thermo-chemical energy storage applications for solar buildings, Sol. Energy. 173 (2018) 1278–1286. doi:10.1016/j.solener.2018.08.075.

[29] L. Calabrese, V. Brancato, V. Palomba, A. Frazzica, L.F. Cabeza, Assessment of the hydration/dehydration behaviour of MgSO4·7H2O filled cellular foams for sorption storage applications through morphological and thermo-gravimetric analyses, Sustain. Mater. Technol. 17 (2018) e00073. doi:10.1016/j.susmat.2018.e00073.

[30] B. Bolto, M. Hoang, S.R. Gray, Z. Xie, New generation vapour permeation membranes, Pervaporation, Vap. Permeat. Membr. Distill. (2015) 247–273. doi:10.1016/B978-1-78242-246-4.00009-X.

[31] A.K.S. Chesterton, D.A.P. De Abreu, G.D. Moggridge, P.A. Sadd, D.I. Wilson, Evolution of

cake batter bubble structure and rheology during planetary mixing, Food Bioprod. Process. 91 (2013) 192–206. doi:10.1016/j.fbp.2012.09.005.

[32] H.A. Sturges, The Choice of a Class Interval, J. Am. Stat. Assoc. 21 (1926) 65–66. doi:10.2307/2965501.

[33] L. Calabrese, L. Bonaccorsi, P. Bruzzaniti, A. Freni, E. Proverbio, Morphological and functional aspects of zeolite filled siloxane composite foams, J. Appl. Polym. Sci. 135 (2018) 45683. doi:10.1002/app.45683.

[34] H. Yu, Z. Guo, B. Li, G. Yao, H. Luo, Y. Liu, Research into the effect of cell diameter of aluminum foam on its compressive and energy absorption properties, Mater. Sci. Eng. A. 454–455 (2007) 542–546. doi:10.1016/j.msea.2006.11.091.

[35] M. Richter, E.M. Habermann, E. Siebecke, M. Linder, A systematic screening of salt hydrates as materials for a thermochemical heat transformer, Thermochim. Acta. 659 (2018) 136–150. doi:10.1016/j.tca.2017.06.011.

[36] Y.N. Zhang, R.Z. Wang, Y.J. Zhao, T.X. Li, S.B. Riffat, N.M. Wajid, Development and thermochemical characterizations of vermiculite/SrBr 2 composite sorbents for low-temperature heat storage, Energy. 115 (2016) 120–128. doi:10.1016/j.energy.2016.08.108.

[37] Y.J. Zhao, R.Z. Wang, Y.N. Zhang, N. Yu, Development of SrBr2 composite sorbents for a sorption thermal energy storage system to store low-temperature heat, Energy. 115 (2016) 129–139. doi:10.1016/J.ENERGY.2016.09.013.

[38] G. Firpo, E. Angeli, L. Repetto, U. Valbusa, Permeability thickness dependence of polydimethylsiloxane (PDMS) membranes, J. Memb. Sci. 481 (2015) 1–8. doi:10.1016/J.MEMSCI.2014.12.043.

[39] P. D'Ans, O. Skrylnyk, W. Hohenauer, E. Courbon, L. Malet, M. Degrez, et al., Humidity dependence of transport properties of composite materials used for thermochemical heat storage and thermal transformer appliances, J. Energy Storage. 18 (2018) 160–170. doi:10.1016/J.EST.2018.04.027.

[40] A. Frazzica, A. Freni, Adsorbent working pairs for solar thermal energy storage in buildings, Renew. Energy. 110 (2017) 87–94. doi:10.1016/j.renene.2016.09.047.

[41] A.R.J. Hussain, A.A. Alahyari, S.A. Eastman, C. Thibaud-Erkey, S. Johnston, M.J. Sobkowicz, Review of polymers for heat exchanger applications: Factors concerning thermal conductivity, Appl. Therm. Eng. 113 (2017) 1118–1127. doi:10.1016/J.APPLTHERMALENG.2016.11.041.

[42] M.P. Wolf, G.B. Salieb-Beugelaar, P. Hunziker, PDMS with designer functionalities—Properties, modifications strategies, and applications, Prog. Polym. Sci. 83 (2018) 97–134.

doi:10.1016/J.PROGPOLYMSCI.2018.06.001.

[43] T. Trantidou, Y. Elani, E. Parsons, O. Ces, Hydrophilic surface modification of PDMS for droplet microfluidics using a simple, quick, and robust method via PVA deposition, Microsystems Nanoeng. 3 (2017) 16091. doi:10.1038/micronano.2016.91.